# Weakening the C-C bond: On the behavior of glyoxylic acid on Pt(111) and its vicinal surfaces

Ricardo Martínez-Hincapié[a],Rosa M. Arán-Ais[a]*, Juan M. Feliu[a]*

[a]*Instituto de Electroquímica, Universidad de Alicante, Apdo. 99, E-03080 Alicante, Spain*

## Abstract

Adsorption and oxidation of glyoxylic acid (GA) on platinum single crystals wereinvestigated by spectroelectrochemical techniques. Among basal planes, Pt(111) is taken as a model surface for reactivity studies in order to point out the C-C bond breaking.For a standard GA concentration (0.1 M), self-poisoning by adsorbed CO ($CO_{ads}$) is the main process dominating the positive-going sweep. The presence of {110} steps on (111) terraces contribute in theC-C bond cleavage, leading toCO formation, while (100) steps do not show a significant effect. Poisonstripping allows GA oxidation in a lower potential range in the negative-going sweep. By working with different GA concentrations ($10^{-5}$ – 0.1 M), surface blockage is hindered, pointing outan alternative reaction pathway, where GA is oxidized in a poison-free surface. Fourier transform infrared spectroscopy (FTIR) experiments allowed the identification of $CO_2$, formic (FA) and oxalic acid (OA) as main products of GA oxidation. We highlight an activity peak at 0.01 M GA, concomitant tothe presence of $CO_2$absorption bands at lower potentials (0.2 V). The formation of $CO_2$ at potentials where CO cannot be oxidized suggests a change in the preferential reaction pathway, where GA is completely oxidized through an active intermediate distinct to $CO_{ads}$.

**Keywords:**Glyoxylic Acid; Platinum single crystal electrodes; Stepped surfaces; In situ FTIR

Corresponding authors: rosa.aran@ua.es; juan.feliu@ua.es

# Introduction

Over the past decades, the electro-oxidation of alcohols has attracted much attention in electrocatalysis since these compounds feed the anodes of direct alcohol fuel cells (DAFC) and can be used in the electrochemical synthesis of different substances[1-3]. In the case of ethanol (EtOH) oxidation reaction (EOR), acetic acid formation through the 4e path predominates against the most desirable 12e path leading to $CO_2$ as final product. The later route can be favored by weakening the C-C bond by placing electron abstractor groups in the molecule, as has been previously demonstrated for ethylene glycol[4]. In the same way, glycolic acid can be oxidized at platinum (Pt) electrodes at low temperature and concentrations[5], in contrast to the aforementioned acetic acid.

Several studies have been carried out on the electrochemistry of glyoxylic acid (GA) on polycrystalline surfaces of different electrode materials such as vitreous carbon[6], gold[7],palladium[8] and platinum[9-11]. The effect of the crystallographic orientation is fundamental from an electrocatalytic point of view, and although GA oxidation was found to be structure sensitive on Pt[11], in situ studies about GA adsorption and reactivity at well-defined metal/solution interfaces are rather scarce[7, 11]. In this sense, and owing the complexity of the GA oxidation reaction, the use of single crystal electrodes is expected to overcome some of the difficulties relatedto the heterogeneity of polycrystalline electrodes, being a powerful tool to understand the catalytic process from a simplified point of view. Moreover, adsorption and oxidation processes can be evaluated by combining cyclic voltammetry with *in situ* infrared measurements.

The complete oxidation of GA leading to $CO_2$ as final product is a 4e process:

$$CHO\text{-}COOH + H_2O \rightarrow 2CO_2 + 4e^- + 4H^+ \qquad (1)$$

Literature reports a double-path mechanism for GA oxidation on Ptsurfaces, in whichthe direct oxidation through an active intermediate competes with the formation of poisoning

intermediates (PI) that strongly adsorb on the surface. These adsorbed species were suggested to be $(CO\text{-}COOH)_{ad}$[12] from the incomplete oxidation of the GA molecule, and $CO_{ad}$ coming from the dissociative adsorption of GA, this later reactionpointing out the breaking of the C-C bond when the GA molecule contacts the Ptsurface. All these studies were performed on concentrated solutions of GA and even in the presence of anions (namely, sulfates) that compete with the adsorption sites on the surface. However, nothing has been reported about the behavior of this molecule at low concentrations using perchloric acid as supporting electrolyte, where competitive anion adsorption is absent. In addition, working with diluted solutions can be useful to favor a particular pathamong other parallel routes with complex reaction schemes.

In the present work we aim to study the surface reactivity, namely the adsorption and oxidation of GA on Ptsingle crystal electrodes, with basal orientations and stepped surfaces vicinal to Pt(111). For this basal plane electrode, Fourier transform infrared spectroscopy (FTIR) in its external reflection configuration has been used to identify the intermediates and products of this reaction at different concentrations. The results here reported show the structure sensitivityof the reactionand the key role that the anolyte concentration plays in order to achieve itscomplete oxidation to $CO_2$.

## Experimental

Pt single crystal surfaces were used as working electrodes and were prepared following standard procedures described elsewhere[13]. Before each experiment, the single crystal electrodes were flame-annealed, cooled down in a reductive atmosphere ($H_2$ + Ar in a 1:3 ratio) and quenched in ultrapure water in equilibrium with this atmosphere before transferring to the electrochemical cell. Preliminary experiments were carried out at room temperature (RT) in a classical two-compartment electrochemical cell, using a Pt wire (99.99 %) as counter electrode and a reversible hydrogen (Air Liquid, N50) electrode (RHE) connected to the cell through a Luggin capillary. Solutions were de-aerated by bubbling Ar (Air Liquid, N50), and were prepared from

perchloric acid (Merck Suprapur) and GA (Sigma Aldrich, 99 %) in ultrapure water from Elga, 18.2 MΩ cm. The electrode potential was controlled using an EG&G PARC 175 signal generator in combination with an eDAQ EA 161 potentiostat and currents were recorded using an eDAQ e-corder ED401 recording system.

Electrochemicalcharacterization of the intermediates on GA oxidation was carried out using a flow cell, which in addition to the components of classical electrochemical cell, has an inlet and outlet through which the solution can be changed while controlling the electrode potential. The key point of this experiment is to control the cleanliness of the cell during the whole procedure.

Further information was gained from spectroelectrochemical experiments, performed with a Nicolet Magna 850 spectrometer equipped with a MCT detector. The spectroelectrochemical cell was provided with a prismatic $CaF_2$ window beveled at 60 º. Unless otherwise stated. spectra shown are composed of 100 interferograms collected with a resolution of 8 $cm^{-1}$ and p polarized light. They are presented as absorbance, according to $A=-\log(R/R_0)$ where $R$ and $R_0$ are the reflectance corresponding to the single beam spectra obtained at the sample and reference potentials, respectively. All spectroelectrochemical experiments were carried out at RT, with a RHE and a Pt wire used as reference and counter electrodes, respectively.

## Results and discussion

### Standard Cyclic Voltammetry on Basal Orientations

Figure 1A shows the first cycle of the oxidation of GA on Pt(111), Pt(100) and Pt(110) electrodes in a 0.1 M GA + 0.1 M HClO4 solution. In order to preserve the surface structure of the electrodes, the potential range was restricted between 0.05-0.95 V. In the positive-going sweep (solid line), extensive blocking of all surfaces due to strongly adsorbed species is observed. It was found that GA spontaneously dissociates on Pt electrodes yielding CO and other species that block the Pt surface sitessuppressing other reactions at potentials lower than

the potential at which the adsorbed CO ($CO_{ad}$) oxidizes to $CO_2$[11]. This phenomenon is known as "self-poisoning" and also occurs in the oxidation of most small organic molecules aimed for fuel cell applications[14-18]. A significant difference in electrocatalytic activity can be observed when comparing the three basal orientations: following the onset for the PI oxidation, the trend is Pt(110)<Pt(111)<Pt(100).Interestingly, hydrogen adsorption in the low potential region can take place at Pt(100) in a greater extent than on the other basal planes. The nature of the PI will be identified in the following FTIR experiments, but the charge integrated under the PI oxidation peaks ($Q_{PI}$)gets some information (table 1). Comparing these results to those previously reported for CO stripping ($Q_{CO}$) on the different basal planes, we observe that for Pt(100) and Pt(110) electrodes, $Q_{CO}$ and $Q_{PI}$ are rather similar, pointing out that for a standard GA solution (0.1 M), the PI is chiefly $CO_{ad}$. Interestingly, for Pt(111) $Q_{PI}$< $Q_{CO}$, indicating that the self-poisoning rate for this surface orientation is smaller. This situation was also found for formic acid[19], ethanol[20] and ethylene glycol[17].In the negative-going sweep (dashed line), the observed oxidation process would correspond to the oxidation of GA on a poison-free Pt surface. As can be seen, the GA oxidation takes place on Pt(100) at an almost negligible rate, while on Pt(110) occurs in a wide potential range. On Pt(111), a symmetrical peak between 0.40 and 0.60 V is recorded.

**Table 1.**Charges comparison for the Pt basal planes[21-26].

| **Electrode** | **$Q^e_{Pt}$*/ μC·cm$^{-2}$** | **$Q_{CO}$ / μC·cm$^{-2}$** | **$Q_{PI}$ / μC·cm$^{-2}$** |
|---|---|---|---|
| **Pt(111)** | 241 | 350-409 | 218 |
| **Pt(100)** | 209 | 306-390 | 302 |
| **Pt(110)** | 148 | 290 | 280 |

**$Q^e_{Pt}$** = theoretical charge assuming one electron per surface Pt atom.

In the present work we have focused on the electrocatalytic behavior of Pt(111). This surface has shown the lower self-poisoning rate and the ability of oxidizing GA in a wider potential range. In addition, Pt(111) is also the most reluctant to produce $CO_2$ from ethanol and its derivates[5, 16, 17]. In this regard, figure 1B displays the evolution of the GA oxidation profile on Pt(111) with successive voltammetric cycles. The amount of charge corresponding to the poison

oxidation around 0.78 V and GA oxidation at 0.48 V decreases upon cycling, while the initially blocked hydrogen adsorption region ($H_{upd}$) is progressively recovered. Nevertheless, the total charge for a Pt(111) electrode in perchloric acid (160 $\mu C \cdot cm^{-2}$ after classical double layer correction[27]) in this region is never achieved. These results point out the existence of another kind of specie(s) (which probably maintains the C-C bond) that adsorbs strongly enough to avoid CO adsorption, but allowing the access for adsorption of hydrogen to the electrode surface. This residue would be originated in the GA oxidation in the negative-going sweep, and its oxidation-desorption would take place at potentials higher than the CO stripping, since its accumulation is observable with repeated potential cycling. Further *in situ*voltammetric and FTIR experiments would help to identify these intermediate species.

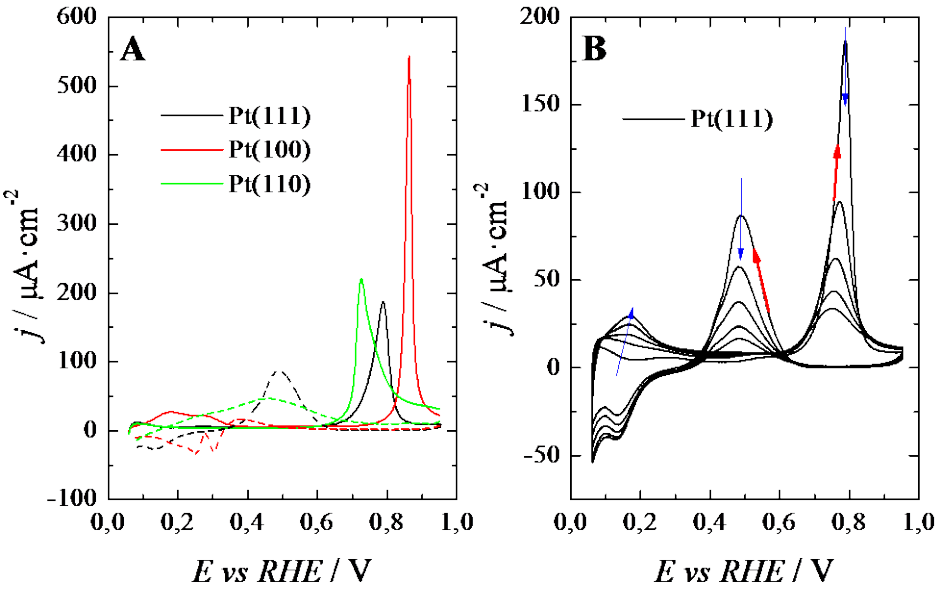


**Figure 1.** (A) Cyclic voltammograms for Pt(111), Pt(100) and Pt(110) electrodes in 0.1 M GA + 0.1 M $HClO_4$. (B) Evolution of the Pt(111) voltammetric profile with successive potential cycles. Red arrows point out the sweep direction; blue arrows indicate the evolution of the different features. Sweep rate, 50 mV $s^{-1}$.

**Cyclic Voltammetry on Stepped Surfaces**

It has been previously reported the effect of steps sites in breaking the C-C bond of ethanol and ethylene glycol molecules[4, 28, 29].Figure 2 shows the GA oxidation on platinum surfaces with n-atom wide (111) terrace orientation separated by monoatomic steps with {100} or {110} symmetry.As can be seen in figure 2A, the voltammetric profile does not substantially change from Pt(111) after the insertion of {100} steps (n>9);the current density of both oxidation peaks decreases as the step density increases, being both signals almost negligible for the surfaces with narrow (111) terraces (n<6). Interestingly, the behavior of the surface corresponding to the turning point, Pt(311), is rather similar to the response of Pt(100) (figure 1A). These results suggest that GA oxidation does not take place on terraces or sites with (100) symmetry, being the C-C splitting and CO formation more difficult also on this surface orientation. On the other hand, figure 2B shows that {110} step sites are more active than {100} sitesfor GA oxidation and the cleavage of the C-C bond through the formation of $CO_{ad}$. This effect is not so clearly observed for surfaces with wide (111) terraces (n>14), where the intensity of both peaks drops as the terrace width decreases, remaining almost constant independently of the step density. Nevertheless, for surfaces with narrower (111) terraces (n<10), the voltammetric responsesinterestingly evolveback to the initial Pt(111) profile. However, the surface corresponding to the turning point, Pt(331), breaks this trend. Unfortunately, the extremely high step density of this kind of electrodes makes their behavior unpredictable. The onset of GA oxidation, however, seems to be almost independent of the symmetry of the defects inserted between the (111) terraces.

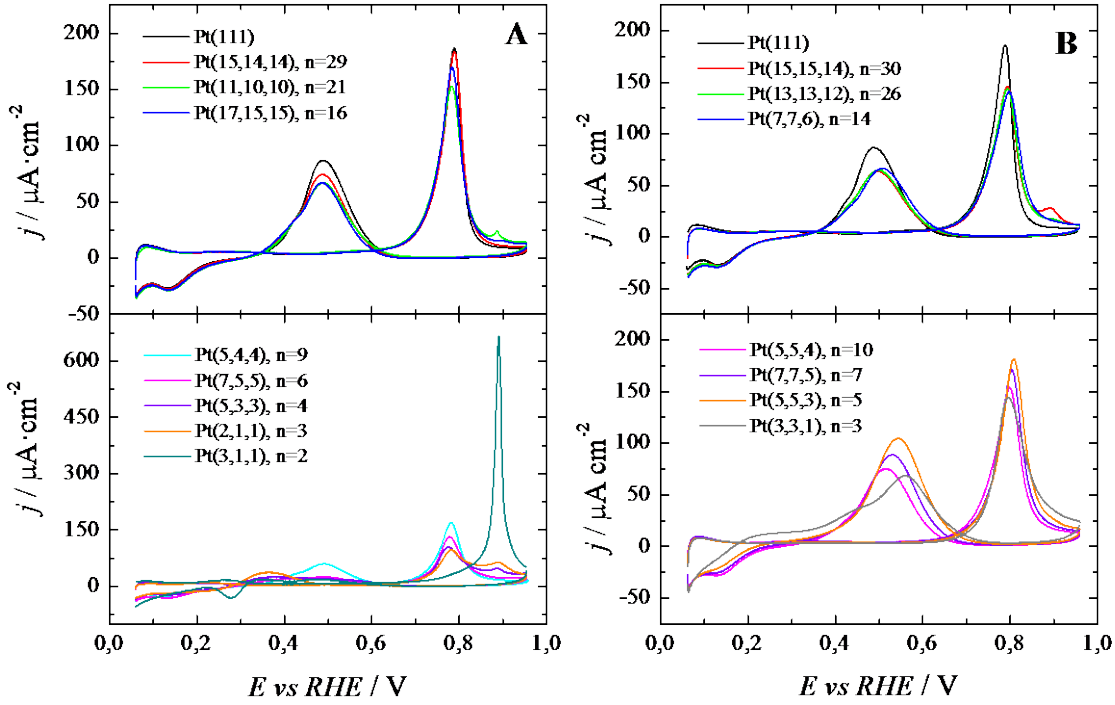


**Figure 2.** Cyclic voltammograms for Pt(111) and its vicinal surfaces with monoatomic steps of (A) (100) and (B) (110) symmetry in 0.1 M GA + 0.1 M $HClO_4$ solution. Sweep rate, 50 mV $s^{-1}$.

## Effect of Glyoxylic Acid Concentration

It is well documented that the relative amount of products depends on ethanol concentration[30]. Thus, similar behavior could be expected for GA.Figures1 and 2 have shown that for a standard GA concentration (0.1 M), the surface blockage by $CO_{ad}$ hinders GA oxidation in the positive-going sweep. However, once the PI has been stripped away, the GA oxidation can take place in a low potential range. Therefore, finding a situation where the GA molecule couldreact on a poison-free surface would be desirable in energy applications. In this regard, it has been previously reported that by working with low concentrated solutions is possible to avoid the self-poisoning of the surface and favour the C-C breaking[4]. Figure 3 shows the voltammetric profile of GA oxidation on Pt(111) upon successive cycling in a more diluted solution (0.01 M GA + 0.1 M $HClO_4$). Several differences can be observed in comparison with figure 1B: i) an oxidation peak in the hydrogen adsorption region, centered at 0.22 V, ii) a pre-wave at 0.58 V

that precedes the (iii) poison-oxidation peak at 0.75 V, and (iv) the GA oxidation feature that takes place at 0.51 V in the negative-going sweep.The oxidation signal that appears at low potentials is only observed in the first cycle, giving way to a stable and partially blocked $H_{upd}$ region.Interestingly, the intensity of the PI stripping peak increases in the second voltammetric cycle, meaning that the species stripped at low potentials in the first cycle partially hinders the CO adsorption. Unlike what observed for the 0.1 M GA solution, the surface is not completely blocked by CO, which allows the GA oxidation in the positive-going sweep (pre-wave signal at 0.5-0.6 V).The evolution of the oxidation profile follows the same trend that figure 1B: all peaks progressively diminish and shift towards more positive potentials until a stable profile is reached, pointing out the accumulation of strongly adsorbed species on the surface.

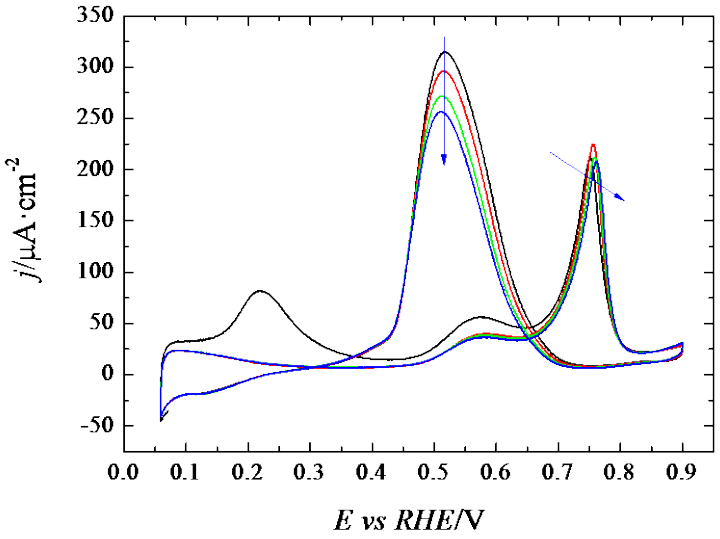


**Figure 3.** Evolution of the Pt(111) voltammetric profile with successive potential cyclesin a 0.01 M GA + 0.1 M $HClO_4$ solution. Arrows indicate the evolution of the different features. Sweep rate, 50 mV $s^{-1}$.

In order to study the effect of GA concentration on its overall oxidation mechanism, further experiments in more diluted solutions were carried out. Figure 4 shows representative voltammetric profiles forPt(111) electrode on pure 0.1 M$HClO_4$and solutions with increasing GA concentrations from $10^{-5}$ to $10^{-3}$ M. A relatively high sweep rate (50 mV·$s^{-1}$) was selected to

discriminate between thermodynamic (adsorption/desorption states) and kinetic processes (oxidation of GA and its intermediates). In contrast with what happened previously, the curves recorded in more diluted solutions overlap nicely in the $H_{upd}$ region (at E<0.3 V), and only at $10^{-3}$ M, this region starts to be distorted. Two possible processes can explain this fact: i) the C-C cleavage through the CO formation does not take place on GA solutions with concentration lower than $10^{-3}$ M, ii) the CO formed from GA decomposition rapidly oxidizes to $CO_2$. Besides the hydrogen adsorption/desorption, the apparition and evolution of other features can be remarked. From the blank profile to the voltammetric profile corresponding to the $2 \cdot 10^{-5}$ M solution, a quasi-reversible peak at around 0.43 V can be observed, which resembles the reversible adsorption/desorption of anion-like species as in the case of glycolic or oxalic acids. At higher potentials, the OH adsorption/desorption region is progressively altered by the presence of GA, being the butterfly peak[31] successively suppressed and shifted towards higher potentials. This later feature is completely lost at $5 \cdot 10^{-5}$ M and higher concentrations. The intensity of the peak at 0.43 V in the positive-going sweep progressively increases with GA concentration, as well as the current intensity around 0.75 V (previously related to the PI oxidation). On the contrary, the signal taking place in the same potential region butin the negative-going scan completely transforms from a desorption state to an oxidation peak that increases and shifts towards lower potentials with increasing GA content in solution.

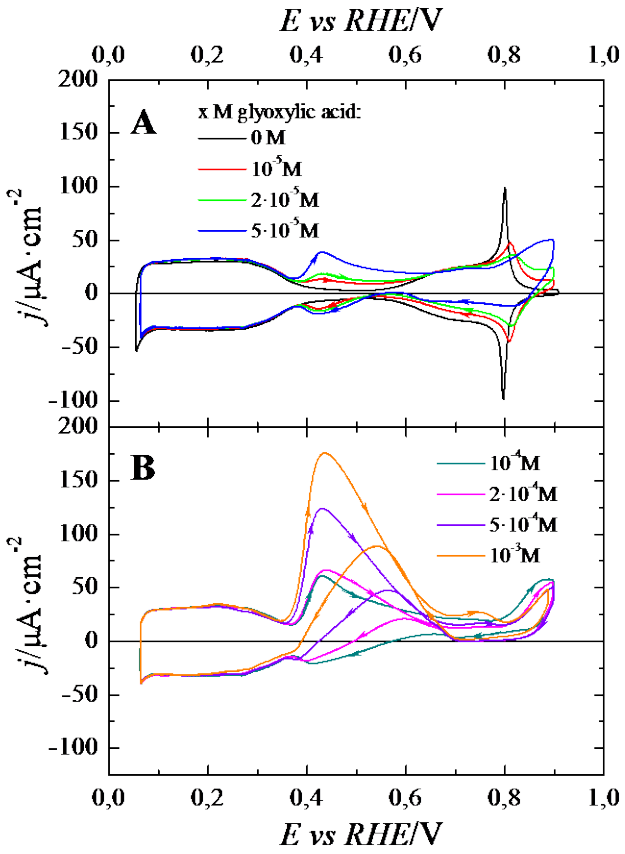


**Figure 4.** Voltammetric behavior of Pt(111) in 0.1 M $HClO_4$ with different concentrations of GA. Arrows point out the sweeping direction. Scan rate: 50 $mV \cdot s^{-1}$.

In this regard, the subtraction of the blank to the curves at different GA concentrations was performed to discriminate between the contributions due to the adsorption/desorption of the ions coming from the supporting electrolyte, and those deriving from the GA adsorption and oxidation (figure 5). Since the $H_{upd}$ region remains almost unaltered for all diluted concentrations, no net current is observed at potentials below 0.3 V.It should be mentioned that, in the absence of self-poisoning process,glyoxylate anions (or derivates) do not block the hydrogen region because the potential of zero charge ($E_{ptzc}$) for the Pt(111) is 0.34 V[32, 33].In the positive scan (figure 5A), the intensity of the signal that appears at 0.43 V gradually increases with GA concentration, indicating that an oxidation process is probably taken place. The drop in the intensity of these peaks might be caused by the adsorption of some by-products generated in

these oxidations. The duality of this process (adsorption/oxidation) is clearly observed when the negative scan is considered (figure 5B): at the lowest concentrations, desorption of an anion is observed, but the current signal of this feature is inverted for higher GA contents, clearly related to GA oxidation. In addition, the butterfly peak associated to the OH adsorption on Pt(111) is partially (or completely) blocked both in the positive and negative going sweeps, indicating the presence of other specie(s) (already present in the solution or coming from GA oxidation) on the surface that inhibit OH adsorption.

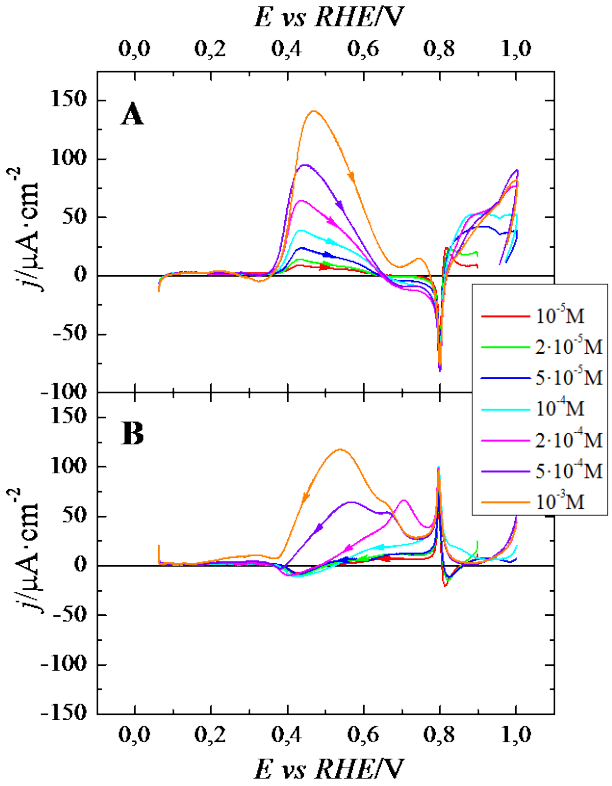


**Figure 5.** Curves resulted from the subtraction of the Pt(111) voltammetric profile on 0.1 M $HClO_4$to the cyclic voltammograms recorded in 0.1 M $HClO_4$ + x M GA. Scan rate: 50 $mV \cdot s^{-1}$.

Interestingly, the voltammetric curves for all concentrations show an increasing current density at potentials higher than 0.9 V, pointing out that another possible reaction can take place if sweeping to higher values. It is reasonable to presume that GA, in a first stage, would oxidize to oxalic acid (OA) in a 2e transfer process:

$$CHO\text{-}COOH + H_2O \rightarrow HOOC\text{-}COOH + 2e^- + 2H^+ \quad (2)$$

In this regard, Orts et al. showed that at standard GA concentration (0.1 M) and in the presence of specific adsorption of sulfates, GA oxidation takes place mainly at potentials higher than 1.0 V[11]. On the other hand, Berna et al. found that the irreversible oxidation of OA (0.01 M) takes place around 1.0 V[34, 35]. In order to get deeper insight into the processes taking place at higher potentials and with the aim of comparing the voltammetric behavior of both GA and OA, the oxidation of diluted solutions of these molecules was studied in a wider potential window (figure 6). The upper limit potential was limited to 1.2 V, where it is well-known that the surface structure of the Pt(111) is preserved[36, 37]. Interestingly, for a concentration of $5 \cdot 10^{-5}$ M (figure 6A), the oxidation profile of both molecules overlap at potentials above 0.8 V, highlighting the partial oxidation of GA to OA at potentials slightly higher than 0.4 V. This similarity is more evidenced in the negative going sweep, where the anion desorption at 0.43 V concurs in both curves. It is worth noting that, after the oxidation process at 0.93 V it is possible to observe the oxidation of the surface, although the blank profile is not completely recovered, thus pointing out the presence of specie(s) that partially block the surface. When the concentration is increased up to $5 \cdot 10^{-4}$ M (figure 6B), the differences between both voltammetric profiles are significant, indicating that beyond the GA oxidation to OA, other reactions are taking place.The most interesting fact is the possibility of oxidize GA in both positive and negative going sweeps while preserving the $H_{upd}$ region unaltered.

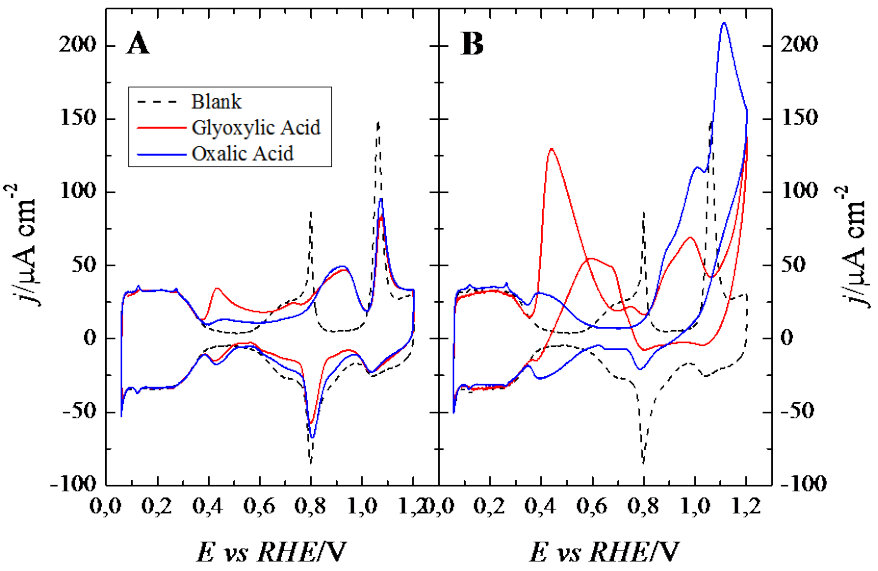


**Figure 6.** Voltammetric profiles for Pt(111) in 0.1 M $HClO_4$(black, dashed line), and solutions containing GA (red line) and OA (blue line) at different concentrations: (A) $5 \cdot 10^{-5}$ M, (B) $5 \cdot 10^{-4}$ M. Scan rate: 50 $mV \cdot s^{-1}$.

With the aim of providing some evidence on what was previously exposed, the charge involved under the feature taking place around 0.43 V in the positive-going sweep was integrated, for both GA ($Q_{GA}$) and OA ($Q_{OA}$) solutions with different concentrations. The obtained results are displayed in table 2. Taking into account the similarity between GA and OA molecules, and assuming that they adsorb in a similar way leading to comparable coverages, it is possible to conclude from the resulting charges ($Q_{GA}$ vs $Q_{OA}$) that both adsorption and oxidation process are taking place in GA solutions.

**Table 2.** Charges comparison for Pt(111) in different GA and OA solutions.

| Concentration / M | $Q_{GA}$ / μC·cm$^{-2}$ | $Q_{OA}$ / μC·cm$^{-2}$ |
|---|---|---|
| **$10^{-5}$** | 3.5 | 0.9 |
| **$5{\cdot}10^{-5}$** | 45.7 | 5.6 |
| **$10^{-4}$** | 126.8 | 27.4 |
| **$5{\cdot}10^{-4}$** | 318.8 | 38.5 |
| **$10^{-3}$** | 493.4 | 41.9 |

**Effect of "Time Contact" in the PI Formation**

One important parameter that controls the amount of species adsorbed on the electrode's surface is the exposure time between the electrode and the solution before the voltammetric experience starts. In this regard, several experiments with different contact periods at a fixed potential (0.3 V) were carried out in a $5{\cdot}10^{-4}$ M GA + 0.1 M $HClO_4$ solution.This potential (0.3 V), close to the $E_{ptzc}$, was chosen to enable both the CO and other intermediates adsorption, and therefore study which is the reaction path that predominates. The ¨time contact¨ experiments were performed as follows: After register a blank to check the cleanliness of the solution and the state of surface, the electrode is holding a fixed potential (0.3 V) for different times to allow the adsorption of the PI, then the voltammetry is register normally. Between each experiment the electrode is flame annealing to ensure the same surface state for all experiments. From figure 7, three facts can be observed: i) the voltammetric peak at 0.43 V, previously assigned to both GA adsorption and oxidation, shifts towards more positive potentials as the exposure time increases, but its intensity remainsalmost constant, ii) the charge involved in the oxidation peak at 0.73 V increases with the contact lapse, but the peak potential ($E_{peak}$) remains almost invariable, and iii) the oxidation peak that takes place in the negative-going sweep also occurs always at the same potential (0.52 V) but with slightly greater intensity as the exposure time is longer.The second fact can be explained considering that the peak intensity ($i_{peak}$) depends on the GA

concentration, which basically remains constant. Regarding the $E_{peak}$ shifting, we must keep in mind that when the $E_{peak}$ of a process is displaced towards higher potentials, it means that the activation energy of this reaction is changing due to a modification of theelectronic structure of the surface, caused in this case by the adsorption of the intermediate species. Assuming a constant coverage of anions coming from GA adsorption and decomposition (reversible process), higher adsorption times would generate greater amounts of CO, adsorbed between the sites occupied by the anions, which would hinder their adsorption and oxidation. Actually, this would also explain the increasing charge involved in the oxidation process at 0.73 V. The progressive blockage of the $H_{upd}$ area at the adsorption potential with increasing contact times also supports this idea.Therefore, the adsorption of the intermediates generating current at low potentials would be a process with faster kinetics than CO formation. However, as soon as this later poison is generated, it would be adsorbed on the surface of the electrode, blocking the active sites for the anion adsorption and subsequent oxidation, thus shifting this peak towards more positive potentials. Finally, concerning the oxidation process taking place in the negative-going sweep, the slightly augment observed in the $i_{peak}$ would suggest that the stripping peak at 0.73 V would not only correspond to CO oxidation, but also the formation of some by-product that would further oxidize in the negative sweep.

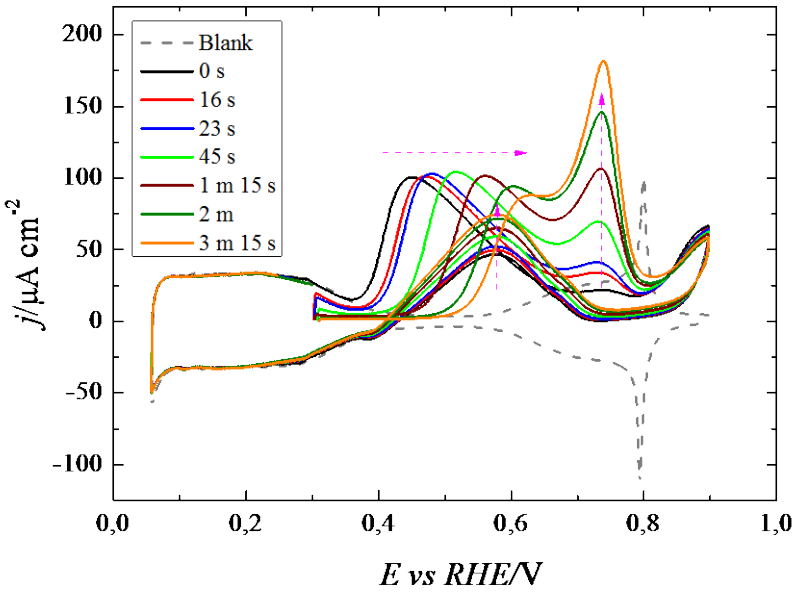

**Figure 7.** Cyclic voltammograms recorded in $5 \cdot 10^{-4}$ M GA + 0.1 M $HClO_4$ for Pt(111). Adsorption potential: 0.3 V. Sweep rate: 50 mV $s^{-1}$.

**Flow Cell Measurements**

With the aim of obtaining information about the intermediates involved in the GA oxidation, experiments using the flow cell configuration where carried out (figure 8). It was previously reported the importance of working with diluted solutions ($<10^{-3}$ M) when using this experimental approach, since all the organic molecules (except those adsorbed on the electrode's surface) must be removed from the cell by flowing the supporting electrolyte[17].The experimental protocol is as follows: initially, the surface structure of the electrode was checked by recording the voltammetric profile in a 0.1 M $HClO_4$ solution. Then, a $10^{-3}$ M GA solution was loaded into the cell, and the adsorption of the intermediate was performed by holding the working electrode potential during3 min at three different values in three sets of experiments: i) 0.2 V, in the $H_{upd}$ zone, ii) 0.4 V, in the double layer region, and iii) 0.6 V, close to the OH adsorption/desorption range.Once the GA solution was removed by flowing the supporting electrolyte, the level of surface blockage was checked in the lower potential range (0.05-0.6 V), and the adsorbed intermediateswere subsequently stripped. Finally, the recovery of hydrogen adsorption capability was monitored.As can be seen, the stripping of the intermediate(s) takes place at 0.7 V when the adsorption potential was 0.2 or 0.4 V, while no oxidation peak is observed when the adsorption is carried out at 0.6 V. It was previously reported that stripping of a CO monolayer at Pt in pure supporting electrolyte requires high potentials (0.7-0.9 V), showing the peak potential a dependence with the CO coverage and the presence of defects on the surface[23, 38-40]. In our case, theintermediate(s) oxidation peak takes place at 0.7 V, suggesting that the species involved in this featureis not only CO, but also other anionic species that strongly adsorb on the surface. The simultaneous adsorption of CO and these anionic species would create a disordered and less compacted CO layer that would oxidize easily (at lower potentials).

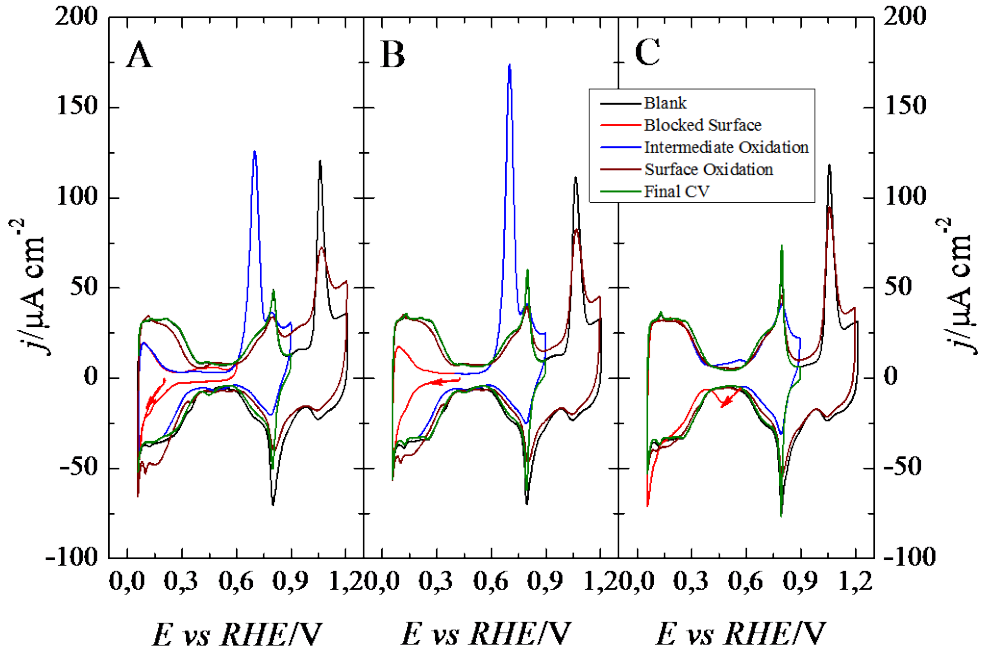


**Figure 8.** Voltammetric oxidation on Pt(111) of the intermediates formed by dissociative adsorption of $10^{-3}$ M GA at (A) 0.2 V, (B) 0.4 V and (C) 0.6 V. Test solution: 0.1 M $HClO_4$. Sweep rate: 50 $mV \cdot s^{-1}$.

Figures 8A and 8B show similar voltammetric responses, independently if the adsorption potential was 0.2 or 0.4 V. In both cases, the 80 % of the charge in the $H_{upd}$ region is suppressed, approximately, but a more intense stripping peak is observed when the adsorption was performed at 0.4 V. The charges integrated for both peaks are 129.3 and 153.2 $\mu C \cdot cm^{-2}$, respectively, lower than those corresponding for pure CO stripping[22, 23].It is possible to explain this fact if we consider that the $E_{ptzc}$ of Pt(111) in perchloric acid medium is 0.34 V, anion adsorption taking place at higher potentials. In this regard, the intermediate(s) stripping feature in figure 8B would contain both CO and other species oxidation. In addition, we found that the recovery of the blank profile was not possible if the upper potential was limited to 0.9 V. This fact points out again that the poisoning intermediate is not only CO, but also specie that adsorbs strongly and suppresses the OH adsorption/desorption. Therefore, 5 cycles up to 1.2 V were performed (in figure 8, only the first cycles are displayed), showing a progressively recovery of the butterfly feature with successive cycling. On the other hand, when the intermediate

adsorption was carried out at 0.6 V (figure 8C) no stripping peak was observed, neither a big distortion of the $H_{upd}$ region, but only an adsorption/desorption peak at 0.47 V in the double layer region and some oxidation around 0.9 V, where OA oxidizes. The anions involved in this signal might be the responsible of the deformation of the OH adsorption/desorption zone.

**Spectroelectrochemical Results**

FTIR experiments were carried out toidentify the species produced on the Pt(111) surface during GA oxidation at different concentrations. The electrode was immersed into the solutionat a controlled potential of 0.1 V. This potential was maintained until the electrode was pressed against the $CaF_2$ window. From that value, the potential was stepped progressively and the different spectra were recorded.In the following spectra,positive bands correspond to the products formed at the sampling potential,while negative bands are due to the consumption of speciespresent at the reference potential (0.1 V). In the case of FTIR measurements, the GA solutions with lower concentrations were studied first for the sake of simplification. In this sense, figure 9 shows the spectra recorded in a $10^{-5}$ M GA solution.The interpretation of the spectra is sometimes difficult when working with such diluted solutions, since the intensity of some bands is comparable to the noise signal. However, three main bands can be observed in the positive-going sweep: i)at 1652 $cm^{-1}$, and (ii) at 1428 $cm^{-1}$, both present in all the potential range, might be related to the characteristic vibrations of GA in solution, and iii) at 1238 $cm^{-1}$, which only appears at potentials above 0.8 V. Since the bending mode of water, $\delta_{OH}$, appears around 1620 $cm^{-1}$, its contribution must be taken into account in the band at 1652 $cm^{-1}$. Nevertheless, the width and the intensity of this band indicate that other vibrations beyond the $\delta_{OH}$ of water are being detected.In this sense, it is important to take into account that in acidic aqueous solution, glyoxylic acid can exist in the hydrated gem-diol[7]:

$$HCO\text{-}COOH + H_2O \rightarrow HC(OH)_2\text{-}COOH \quad (3)$$

whose characteristic vibrations are between 1600-1650 $cm^{-1}$. Hence, we must consider that the characteristic vibrations of either the aldehyde or the diol moieties can also appear in the spectra. The band at 1238 $cm^{-1}$ can be related to some specie that adsorb on the surface on the surface, producing the distortion of the butterfly peak, as aforementioned. IR bands between 1200 and 1400 $cm^{-1}$ are characteristic for the adsorption of carboxylic acids in a bidentate adsorption configuration through the two oxygen atoms of the carboxylic group[34, 41]. Surprisingly, $CO_2$ formation above 0.9 Vis observedby the appearance of a low intensityband at 2345 $cm^{-1}$.In the negative-going sweep, the band of $CO_2$ is present in all spectra, even though at low potentials due to its permanence in the thin layer. Since bands from CO adsorption are not observed, it can be deduced that $CO_2$ is produced from GA (or some of its intermediates) oxidation.

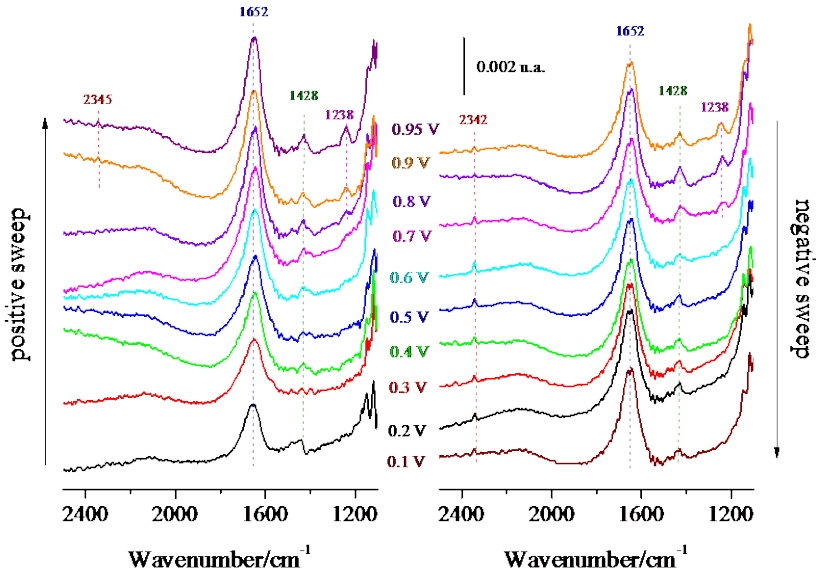


**Figure 9.** Spectra obtained at different potentials, as labeled, for the oxidation of $10^{-5}$ M GA + 0.1 M $HClO_4$ in $H_2O$ at the Pt(111) electrode. The reference spectrum was taken at 0.1 V.

FTIR experiments were also performed in a $10^{-3}$ M GA + 0.1 M $HClO_4$solution (figure 10). The absence of clear $CO_{ad}$ positive bands (which appear around 2040 and 1810 $cm^{-1}$, as will be described below) is also significant in this case. However, a negative band at 2062 $cm^{-1}$ can be observed above 0.6 V, pointing out the existence of little amounts of CO in the reference

spectra. This fact agrees with the little distortion of the $H_{upd}$ region previously observed in the CV. Unlike what described in the previous case (figure 9), no other bands besides the one at 1640 $cm^{-1}$ can be observed below 0.6 V. $CO_2$ formation is triggered above this potential, andit is present in all spectra, even though at low potentials in the negative-going sweep, due to its permanence in the thin layer, as previously mentioned.Nevertheless, the intensity of this band decreases at potentials lower than 0.5 V, which points out that $CO_2$ is diffusing away from the thin layer and no additional $CO_2$ is being formed below this potential. On the other hand, new bands appear at potentials above 0.7 V in the positive-going sweep, which remain in the spectra until they disappear at 0.6 V in the negative-going scan.Thus, positive bands at 1735, 1640, 1529, 1431, 1337 and 1232 $cm^{-1}$ are observed. The signal at 1735 $cm^{-1}$ is typical for the vibration of a carbonyl group, and can be related to symmetric stretching $\nu_s$(C=O) of a carboxylic acid. On the other hand, the signals at 1529 and 1337 $cm^{-1}$ are characteristic of asymmetric ($\nu_{asym}$ OCO) and symmetric ($\nu_{sym}$ OCO) stretching of a deprotonated carboxylic acid. It is worth noting to point out the evolution of the relative intensity of the bands in the region between 1600-1200 $cm^{-1}$at potentials above 0.6 V. These results suggest that above this potential, GA molecules (previously adsorbed or those present in the solution) find a surface free of $CO_{ad}$, thus adsorbing and reacting through the formation of OA (2e process), and further oxidize to $CO_2$.

$$CHO\text{-}COOH + H_2O \rightarrow HOOC\text{-}COOH + 2e^- + 2H^+ \qquad (2)$$

$$HOOC\text{-}COOH \rightarrow 2CO_2 + 2e^- + 2H^+ \qquad (4)$$

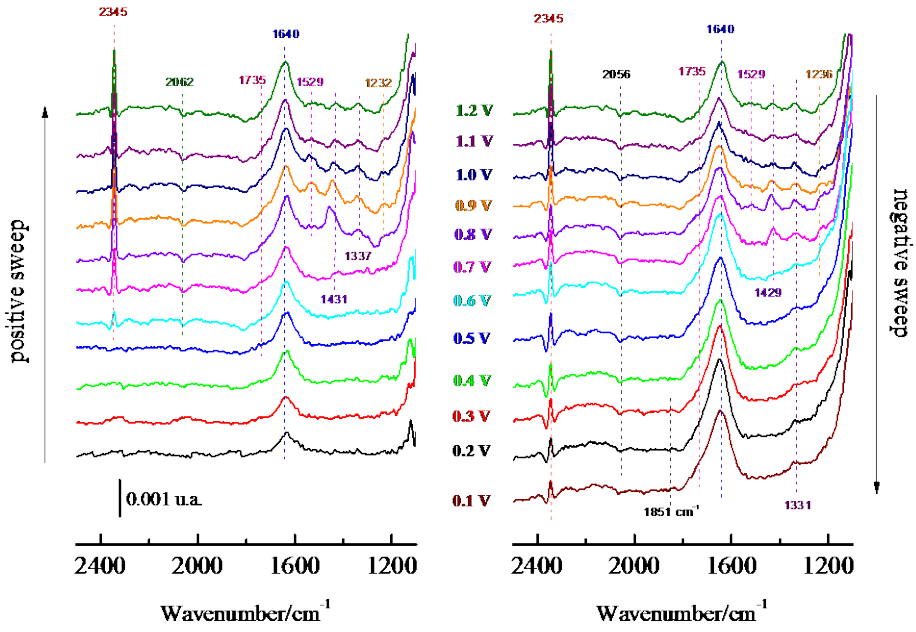


**Figure 10.** Spectra obtained at different potentials, as labeled, for the oxidation of $10^{-3}$ M GA + 0.1 M $HClO_4$ in $H_2O$ at the Pt(111) electrode. The reference spectrum was taken at 0.1 V.

For higher GA concentrations, such as 0.01 and 0.1M (figures11 and 12, respectively), a new situation is found, where adsorbed CO is the main feature in the spectra. In this regard, three major bands can be observed in the spectrain the first stage of the positive-going sweep (0.2-0.5 V): (i) between 2070-2040 and (ii) between1830-1810 $cm^{-1}$, both corresponding to linear and multi-bounded$CO_{ad}$, ($CO_L$) and ($CO_M$) respectively[10], and (iii) around 1640 $cm^{-1}$, related to both the gem-diol vibrations and the $\delta_{OH}$of water,as aforementioned. These results confirm that, for both concentrations, the surface of the electrode is blocked by $CO_{ad}$ at low potentials, and that CO preferentially adsorbs in an*on-top* configuration, as suggested from the relative intensity of the $CO_L$ and $CO_M$ bands. In absence of band coupling conditions[42], $CO_{ad}$ oxidation is triggered above 0.6 V, as deduced from the decrease of the intensity of the corresponding bands while the intensity of the $CO_2$ signal is increased. These results are in agreement with the peak observed in the voltammetric profile (0.65-0.8 V), previously related to the oxidation of the poisoning species. However, the most interesting difference between both concentrations is that, while at 0.1 M GA the $CO_2$generation starts above 0.6 V, for 0.01 M GA $CO_2$ is formed

also at adsorption potentials where adsorbed CO cannot be oxidized (positive-going sweep). Therefore, it must result from direct decomposition of a carboxylic group in contact with the Pt surface to $CO_2$. In this regard, Iwasita et al. showed that $CO_2$ production from 0.025 M ethanol passes through a maximum and then decreases[30]. Our results point out a similar situation in which 0.01 M GAcan completely oxidize at low potentials through the 4e path to $CO_2$.

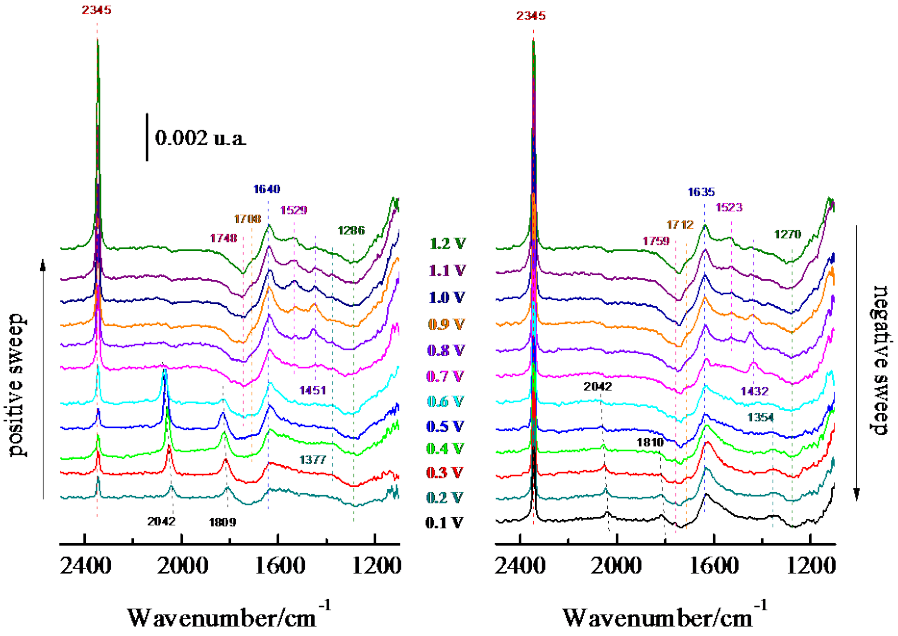


**Figure 11.** Spectra obtained at different potentials, as labeled, for the oxidation of 0.01 M GA + 0.1 M $HClO_4$ in $H_2O$ at the Pt(111) electrode. The reference spectrum was taken at 0.1 V.

In addition, the spectra acquired for the oxidation of 0.01 M GA (figure 11) revealed that the pre-wave observed in the CV at 0.5-0.65 V is not related with the $CO_{ad}$ oxidation, but with the reaction of GA molecules giving rise to other intermediate species. In this potential range, it is possible to observe the bands at 1377 and 1708 $cm^{-1}$, which might be associated to the adsorption of the GA in its gem-diol form, and the band at 1640 $cm^{-1}$, related to its partial oxidation to oxalic acid (equation 2).At high potentials (>0.8 V), independently of the sweep direction, it is possible to observe that, besides the intense band of $CO_2$ production (2345 $cm^{-1}$), GA is being consumed (negative bands at 1759 and 1270 $cm^{-1}$) and some species are produced and adsorbed (positive bands at 1635, 1523, 1432 $cm^{-1}$) on the surface of the electrode. These

species are proposed to be oxalic (1737, 1628, 1308 and 1273 $cm^{-1}$)and formic acid (1330 $cm^{-1}$), whose characteristic bands are found in the spectra[34, 43].Both molecules can be further oxidized to produce $CO_2$, being the adsorbed formiate (coming from the C-C splitting of the GA molecule) an active intermediate to this final reaction.

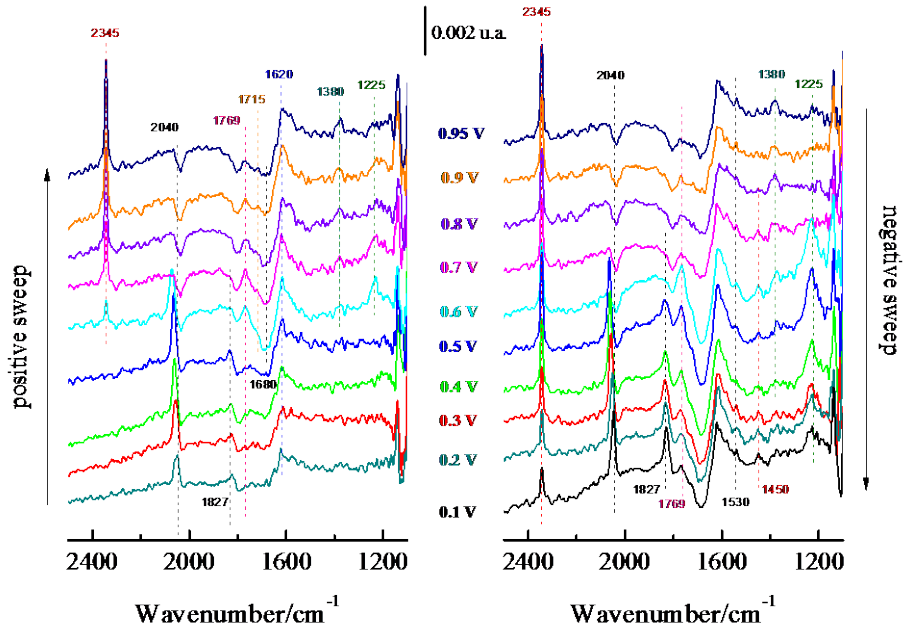


**Figure 12.** Spectra obtained at different potentials, al labeled, for the oxidation of 0.1 M GA + 0.1 M $HClO_4$ in $H_2O$ at the Pt(111) electrode. The reference spectrum was taken at 0.1 V.

Most of the bands observed in the spectra recorded for a 0.1 M GA solution have already been assigned to adsorbed CO (in *on top* and *bridge* configurations), $CO_2$ generation, and the adsorption of molecules with carboxylic groups. Nevertheless, the most notorious feature in these spectra is the negative band at 1680 $cm^{-1}$, which intensity increases with increasing potential, and becoming more pronounced in the negative-going sweep. As before, this negative band must be attributed to the consumption of GA since at high potentials we have a situation where the $CO_{ad}$ has been stripped from the surface, thus the molecules of GA find a clean surface where adsorb and react. At 0.7-0.8 V (onset of the oxidation peak in the voltammetric profile), positive bands at 1769, 1720, 1530, 1450 and 1225 $cm^{-1}$ emerge, while the negative

band at 1680 $cm^{-1}$ becomes more pronounced. As aforementioned, these bands can be related to carboxylic acid vibration modes. On the other hand, CO starts to adsorb again at 0.5 V. All these bands remain in the spectra until the end of the cycle. These results point out that two main processes take place at the surface of the electrode: i) complete oxidation of GA to $CO_2$ via CO poisoning, and ii) partial oxidation giving rise to $C_1$ and $C_2$ molecules, including CO.

Both cyclic voltammetry and FTIR experiments performed at different GA concentrations have demonstrated the accumulation of these species (CO adsorption included) on the surface of the electrode. The characteristic vibrations of the different possible reaction intermediates are rather similar, being difficult to assign the bands to the formation of a particular species at this stage. Nevertheless, we point out the formation of OA and formic acid as active intermediates in the formation of $CO_2$.

## Conclusions

The voltammetric behavior of Pt single crystal electrodes with basal orientations and two series of stepped surfaces for the oxidation of concentrated GA have been studied, showing that the {100} steps on the {111} terraces are not particularly active for this reaction, while the presence of {110} steps enhances the cleavage of the C-C bond through the formation of adsorbed CO. We have found differences in the voltammetric profile of more diluted GA solutions, which display less blockage of the $H_{upd}$ region by $CO_{ad}$ and a pre-wave that precedes the poison oxidation. In this respect, GA adsorption and oxidation is faster than $CO_{ad}$ formation, which requires higher GA concentrations. Moreover, once CO is formed, it adsorbs on the surface thus dominating the reactivity. FTIR experiments have shown that $CO_2$, oxalic and formic acids are the chief products of the oxidation of GA, being these later molecules (principally oxalic acid) accumulated on the surface of the electrode. $CO_2$ is the principal product, even at low potentials, when GA is present in more diluted solutions, showing that working with low concentrations may be a strategy to gain information to develop more efficient fuel cell anodes.

## Acknowledgements

This work was carried out under financial support of MICINN (project no. CTQ2013-44083-P). R.M.H. acknowledges support from GeneralitatValenciana under Santiago Grisolia Program (GRISOLIA/2013/008).

## References

1. Kamarudin, M. Z. F.; Kamarudin, S. K.; Masdar, M. S.; Daud, W. R. W. *Int. J. Hydrogen Energy* **2013,** 38, 9438-9453.
2. Davis, S. E.; Ide, M. S.; Davis, R. J. *Green Chem.* **2013,** 15, 17-45.
3. García-Cruz, L.; Iniesta, J.; Thiemann, T.; Montiel, V. *Electrochem. Commun.* **2012,** 22, 200-202.
4. Arán-Ais, R. M.; Herrero, E.; Feliu, J. M. *Electrochem. Commun.* **2014,** 45, 40-43.
5. Arán-Ais, R.; Herrero, E.; Feliu, J. *J. Solid State Electrochem.* **2015,** 19, 13-21.
6. Pierre, G.; El Kordi, M.; Cauquis, G. *Electrochim. Acta* **1985,** 30, 1219-1225.
7. Delgado, J. M.; Blanco, R.; Pérez, J. M.; Orts, J. M.; Rodes, A. *J. Phys. Chem. C* **2010,** 114, 12554-12564.
8. Ocón, P.; González Velasco, J. *Bull. Electrochem.* **1999,** 15, 543-551.
9. Horányi, G.; Kazarinov, V. E.; Vassiliev, Y. B.; Andreev, V. N. *J. Electroanal. Chem.* **1983,** 147, 263-278.
10. Leung, L. W. H.; Weaver, M. J. *Langmuir* **1990,** 6, 323-333.
11. Orts, J. M.; Feliu, J. M.; Aldaz, A. *J. Electroanal. Chem.* **1993,** 347, 355-370.
12. Kazarinov, V. E.; Vassiliev, Y. B.; Andreev, V. N.; Horányi, G. *J. Electroanal. Chem.* **1983,** 147, 247-261.
13. Clavilier, J.; Armand, D. *J. Electroanal. Chem.* **1986,** 199, 187-200.
14. Boronat-Gonzalez, A.; Herrero, E.; Feliu, J. M. *J. Solid State Electrochem.* **2014,** 18, 1181-1193.
15. Grozovski, V.; Climent, V.; Herrero, E.; Feliu, J. M. *J. Electroanal. Chem.* **2011,** 662, 43-51.
16. Colmati, F.; Tremiliosi-Filho, G.; Gonzalez, E. R.; Berna, A.; Herrero, E.; Feliu, J. M. *Faraday Discuss.* **2008,** 140, 379-397; discussion 417-337.
17. Arán-Ais, R.; Abe Santos, N.; Villulas, H. M.; Feliu, J. M. *ECS Trans.* **2013,** 53, 11-22.
18. Schnaidt, J.; Heinen, M.; Jusys, Z.; Behm, R. J. *J. Phys. Chem. C* **2013,** 117, 12689-12701.
19. Feliu, J. M.; Herrero, E., Formic acid oxidation. In *Handbook of Fuel Cells - Fundamentals, Technology and Applications*, Vielstich, W.; Gasteiger, H.; Lamm, A., Eds. John Wiley & Sons, Ltd.: Chichester, 2003; Vol. 2, pp 625-634.
20. Buso-Rogero, C.; Grozovski, V.; Vidal-Iglesias, F. J.; Solla-Gullon, J.; Herrero, E.; Feliu, J. M. *J. Mater. Chem. A* **2013,** 1, 7068-7076.
21. Korzeniewski, C.; Climent, V.; Feliu, J., Electrochemistry at Platinum Single Crystal Electrodes. In *Electroanal. Chem.*, CRC Press: 2011; pp 75-170.

22. Herrero, E.; Rodes, A.; Perez, J. M.; Feliu, J. M.; Aldaz, A. *J. Electroanal. Chem.* **1995,** 393, 87-96.
23. Farias, M. J. S.; Camara, G. A.; Feliu, J. M. *J. Phys. Chem. c* **2015,** 119, 20272-20282.
24. Gómez, R.; Rodes, A.; Perez, J. M.; Feliu, J. M.; Aldaz, A. *Surf. Sci.* **1995,** 344, 85-97.
25. Cuesta, A. *Electrocatalysis* **2010,** 1, 7-18.
26. Gómez, R.; Feliu, J. M.; Aldaz, A.; Weaver, M. J. *Surf. Sci.* **1998,** 410, 48-61.
27. Clavilier, J.; Albalat, R.; Gómez, R.; Orts, J. M.; Feliu, J. M.; Aldaz, A. *J. Electroanal. Chem.* **1992,** 330, 489-497.
28. Shin, J. W.; Tornquist, W. J.; Korzeniewski, C.; Hoaglund, C. S. *Surf. Sci.* **1996,** 364, 122-130.
29. Tarnowski, D. J.; Korzeniewski, C. *J. Phys. Chem. B* **1997,** 101, 253-258.
30. Camara, G. A.; Iwasita, T. *J. Electroanal. Chem.* **2005,** 578, 315-321.
31. Berna, A.; Climent, V.; Feliu, J. M. *Electrochem. Commun.* **2007,** 9, 2789-2794.
32. Climent, V.; Gómez, R.; Feliu, J. M. *Electrochim. Acta* **1999,** 45, 629-637.
33. Climent, V.; Garcia-Araez, N.; Herrero, E.; Feliu, J. *Russ. J. Electrochem.* **2006,** 42, 1145-1160.
34. Berna, A.; Rodes, A.; Feliu, J. M. *J. Electroanal. Chem.* **2004,** 563, 49-62.
35. Berna, A.; Rodes, A.; Feliu, J. M. *Electrochim. Acta* **2004,** 49, 1257-1269.
36. Bjorling, A.; Herrero, E.; Feliu, J. M. *J. Phys. Chem. C* **2011,** 115, 15509-15515.
37. Gomez-Marin, A. M.; Rizo, R.; Feliu, J. M. *Beilstein J Nanotech* **2013,** 4, 956-967.
38. Feliu, J. M.; Orts, J. M.; Fernández-Vega, A.; Aldaz, A.; Clavilier, J. *J. Electroanal. Chem.* **1990,** 296, 191-201.
39. Wieckowski, A.; Rubel, M.; Gutiérrez, C. *J. Electroanal. Chem.* **1995,** 382, 97-101.
40. Lebedeva, N. P.; Koper, M. T. M.; Herrero, E.; Feliu, J. M.; van Santen, R. A. *J. Electroanal. Chem.* **2000,** 487, 37-44.
41. Heinen, M.; Jusys, Z.; Behm, R. J. *J. Phys. Chem. C* **2010,** 114, 9850-9864.
42. Chang, S. C.; Roth, J. D.; Weaver, M. J. *Surf. Sci.* **1991,** 244, 113.
43. Cuesta, A.; Cabello, G.; Gutierrez, C.; Osawa, M. *Phys. Chem. Chem. Phys.* **2011,** 13, 20091-20095.